Werner Risau Prize 2014
Coupling of angiogenesis and osteogenesis by a specific vessel subtype in bone

Anjali P. Kusumbe

In the mammalian skeletal system, growth of the vascular network is regulated by signals provided by chondrocytes and other bone cells, among which the vascular endothelial growth factor (VEGF) is studied best1. Conversely, blood vessels are thought to influence the osteogenic generation of new bone2. In addition to historic studies highlighting the close proximity of vascular and osteoblastic cells, potential roles of angiogenic blood vessel growth in fracture healing have been proposed3. It also has been suggested that alterations in the skeletal microvasculature might be linked to compromised hematopoiesis and osteogenesis in human subjects with primary osteoporosis or at old age4,5. However, direct evidence for such disease-causing or age-related alterations is lacking and our understanding of the normal organisation, functional specialization and precise function of the skeletal vasculature is incomplete. The precise overall organization of the skeletal vasculature has remained poorly understood because of technical difficulties associated with the processing of bone combined with the loss of crucial 3D information in thin tissue sections. Revised immunohistochemistry protocols have now allowed us to image the bone vasculature at high resolution.

In addition to revised immunofluorescence protocols, we visualised bone vessels with a combination of EC specific, tamoxifen-inducible Cdh5(PAC)-CreERT2 and Rosa26-mT/mG Cre reporter transgenic mice6,7. Imaging of the bone microvasculature with both approaches uncovered structurally distinct capillary subsets. Endothelial tubes in the metaphysis resembled straight columns that were interconnected by distal vessel loops or arches. In contrast, diaphyseal capillaries displayed the highly branched pattern characteristic for the sinusoidal vasculature of bone marrow (Fig. 1a, b). At the interface between metaphysis and diaphysis, the two vessel types were connected confirming that they were part of one continuous vascular bed (Fig. 1b).

The different vessel types were distinguishable by immunostaining with specific cell surface markers. Columnar tubes and arches in the metaphysis and endosteal endothelial cells (ECs) were strongly positive for CD31/PECAM1 and Endomucin (Emcn), while sinusoidal vessels in the diaphysis displayed only weak CD31 staining and slightly lower Emcn expression (Fig. 1c). A distinct CD31hi/Emcnhi endothelial subset could be also identified and separated from CD31lo/Emcnlo cells in single cell suspensions of long bones(Fig. 1d). Quantitative analysis by flow

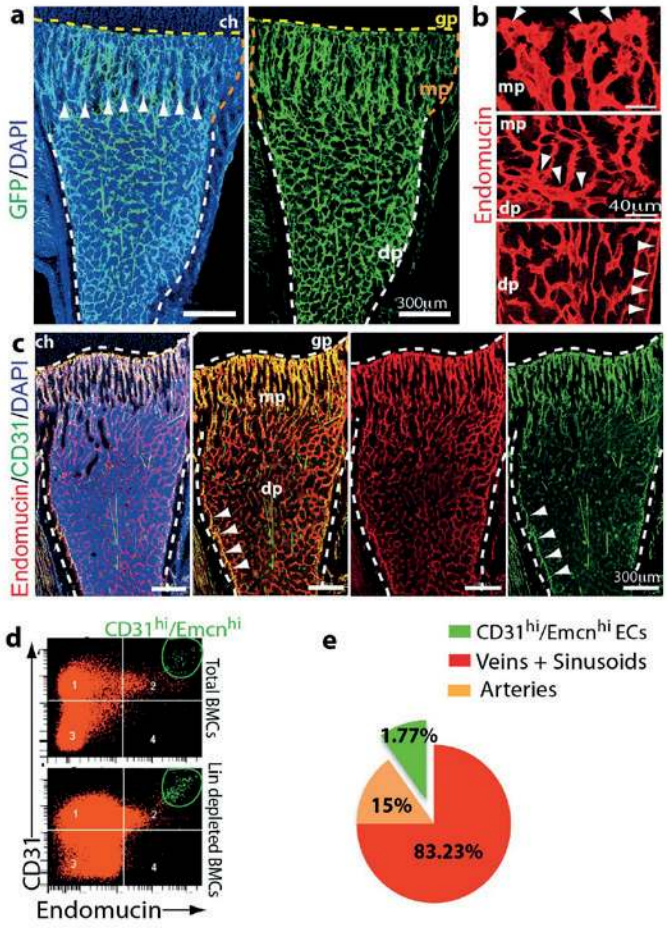

Figure 1. Identification of a distinct vessel subtype in murine bone. a, Representative tile scan confocal images of the GFP+ (green) endothelium in 4 week-old Cdh5(PAC)-CreERT2 x Rosa26-mT/mG double transgenic tibia. Nuclei, DAPI (blue). Yellow dotted line marks growth plate (gp). Note distinct organisation of microvessels in metaphysis (mp) and diaphysis (dp) as well as their connections (arrowheads). b, Maximum intensity projections of Endomucin+ (red) column vessels in metaphysis (mp, arrowheads mark distal protrusions) and highly branched sinusoids in diaphysis (dp). Central panel shows interconnections (arrowheads) between both vessel subtypes. c, Confocal tile scan of 4 week-old tibia images showing distinct patterns of CD31+ (green) and Endomucin+ (red) ECs. Nuclei, DAPI (blue). Strong CD31 and Endomucin signals mark capillaries in metaphysis (mp) and endosteum (arrwoheads). d, Representative flow cytometry dot plots showing the distinct CD31hi Endomucinhi EC subset in lineage (lin) depleted bone marrow cells. e, Pie chart showing the relative abundance of EC subtypes in 4 week-old long bone. CD31hi/Emcnhi cells represent 1.77±0.01% (mean ± s.d.m of 7 mice) of total ECs.

cytometry showed that CD31hi/Emcnhi cells represented only a small fraction of total ECs (Fig. 1e). The observations above established the existence of spatial and phenotypic heterogeneity in the bone endothelium. On the basis of these findings, we propose the following terminology for bone microvessels: type H for the small CD31hi/Emcnhi subset and type L for the CD31lo/Emcnlo sinusoidal vessels.

Immunostaining showed that Osterix+ osteoprogenitors, which will give rise to osteoblasts and osteocytes8, were selectively positioned around type H but not type L endothelium (Fig. 2a). Despite the low frequency (~1.77%) of type H endothelial cells (ECs) in the bone endothelial cell fraction and ~0.015% in total bone marrow (Fig. 1e), the majority of Runx2+ (82.63±1.8%), collagen 1α+ (74±3.3%) and Osterix+ cells (70±1.9%) were located directly adjacent to CD31hi/Emcnhi vessels (Fig. 2b,c).

To understand this distribution pattern of osteoblastic cells, the expression of mRNAs for secreted growth factors with known roles in osteoprogenitor survival and proliferation was analysed in freshly purified ECs from long bone. Pdgfa, Pdgfb, Tgf1, Tgf3, and Fgf1 transcripts were significantly higher expressed in type H relative to type L ECs (Fig. 2c). Accordingly, the two bone capillary EC subsets have specific expression profiles suggesting specialized functional properties.

It has been previously reported that osteoblast numbers declines during aging9. Our analysis of bone endothelium during ageing illustrated pronounced reduction of type H vessels, which were much more abundant in juvenile (4 week-old) mice compared to (11 week-old) adults, and were nearly absent in aged (70 week-old) animals (Fig. 2d). EC proliferation was high within the type H subpopulation in juvenile mice and declined rapidly in adulthood (Data not shown). In contrast, the rate of type L EC proliferation did not differ significantly between juvenile and older animals (Data not shown).

HIF-1α controls physiological and pathological neo-angiogenesis2. To investigate HIF-1α function in the postnatal bone endothelium, inducible EC-specific loss-of-function mice (Hif1aiΔEC) were generated by combining loxP-flanked Hif1a alleles (Hif1alox/lox)10 and Cdh5(PAC)-CreERT2 transgenics. Following tamoxifen administration from postnatal day (P) 10 to P14, analysis of Hif1aiΔEC mutants at P20 revealed striking vascular defects. Type H endothelium was strongly reduced in metaphysis and endosteum (Fig. 3a), the number of diaphyseal type L vessels and ECs was comparable to control littermates.

The von Hippel-Lindau (VHL) E3 ubiquitin protein ligase controls the stability and thereby biological activity of HIF-1α and other substrates11. Inducible, EC-specific targeting of the murine Vhl gene with the same strategy as described above for Hif1a led to pronounced expansion of type H endothelium and metaphyseal vessel columns and the surrounding osteoprogenitors (Fig. 3c,d). Osteoprogenitors were significantly reduced in Hif1aiΔEC samples (Fig. 3a,b).

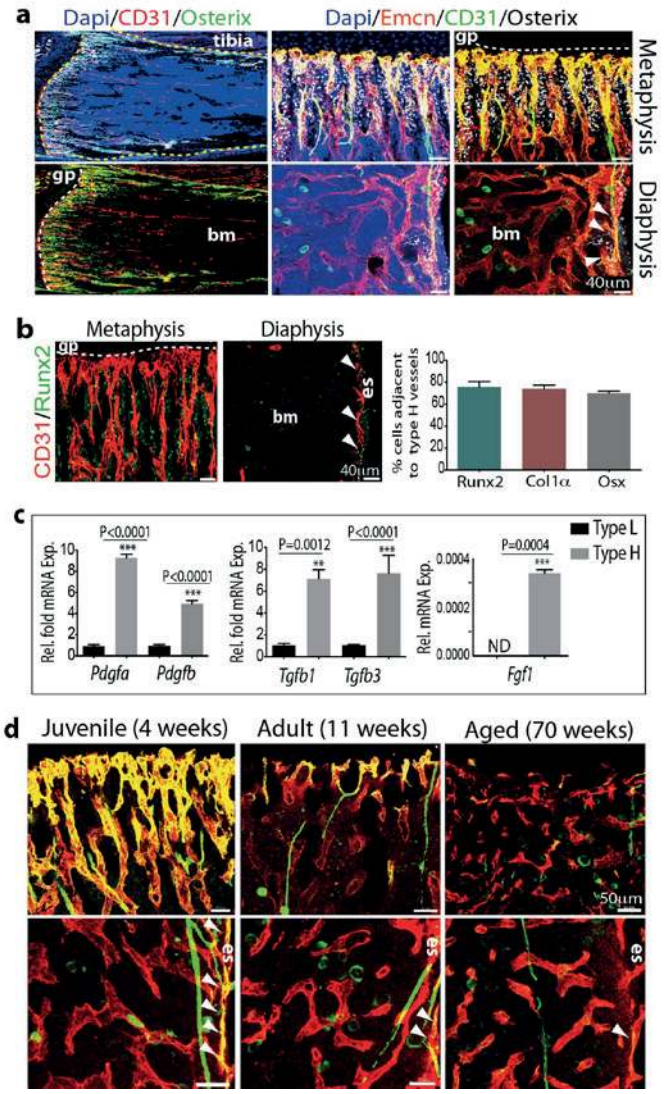

Figure 2. Association of osteoprogenitor cells with type H ECs and decline of type H ECs in aged bones.
a. Confocal images of 4 week-old tibia with the indicated immunostainings. Nuclei, DAPI (blue). Growth plate (gp) and bone marrow cavity (bm) are marked. Osterix+ are found in proximity to CD31hi/Emcnhi (type H) ECs in metaphysis and endosteum (arrowheads). b, Representative confocal images (left panel) of immunostained 4 week-old tibia showing association of Runx2+ osteoprogenitors (green) with CD31+ (red) vessels in metaphysis and endosteum (es). Minimum exposure was used to capture CD31 fluorescence to project only cells with high CD31 intensity. Quantitative analysis (right panel) of proximity (≤20μm) of Runx2+, Collagen1α+ (Col1α) and Osterix+ (Osx) to nearest type H vessel. Mean±s.e.m, n=5. c, qPCR analysis of growth factor expression (normalised to Actb) by CD31hi/Emcnhi ECs relative to CD31lo/Emcnlo ECs sorted from murine tibia. Data represent mean±s.e.m (n=4-6). P values, two-tailed unpaired t-test. d, Representative confocal images of CD31 (green) and Endomucin (red) immunostained tibia sections at 4, 11 and 70 weeks. Note age-dependent decline of CD31hi/Endomucinhi ECs in metaphysis (upper panel) and in endosteal (es, arrowheads) region in diaphysis (lower panel) of bone.

Prolyl-4-hydroxylases (PHDs) modify HIF-1α and thereby mark the protein for degradation under normoxic conditions. Accordingly, PHD inhibitors, such as deferoxamine mesylate (DFM), enhance HIF-1α stability and activity12. Next, we tested whether DFM promotes CD31hi/Emcnhi ECs, neo-angiogenesis and osteogenesis in aged animals. While long bones of aged, 64 to 70 week-old mice treated with vehicle control contained very few CD31hi/Emcnhi vessels, DFM administration led to substantial expansion of type H endothelium (Fig. 3e) and emergence of vessel-associated Osterix+ cells (Fig. 3f). Furthermore, μ-CT examination showed that 6 weeks of DFM treatment led to significantly increased bone mass (Fig. 3g,h). While the activity of DFM is not restricted to ECs and is likely to affect multiple cell populations, the findings above argue for crucial roles of endothelial HIF in controlling bone angiogenesis, type H vessel abundance, endothelial growth factor expression, and osteogenesis.

Above finding that capillaries in the skeletal system of mice can be subdivided into type H and type L endothelium on the basis of morphological, molecular and functional criteria should be hugely beneficial for future studies in basic and medical research. CD31hi/Emcnhi capillaries at the distal end of the arterial network in bone might represent the central building block of a metabolically specialised tissue environment with privileged access to oxygen and nutrients, which is likely to influence the growth potential and metabolism of other cell types. This is not only relevant for osteoblastic cells but potentially also for hematopoietic stem and progenitor cells, which preferentially home to the metaphysis after transplantation13.

We also propose that type H ECs mediate local growth of the vasculature and provide niche signals for perivascular osteoprogenitors. Type H vessel formation and the expression of potential angiocrine factors for osteoblastic cells are enhanced by HIF and by Notch signalling14. Thus, the abundance of CD31hi/Emcnhi ECs may be useful as diagnostic readout for the growth status of the bone vasculature and its pro-osteogenic capacity. Our results also indicate that specific molecular pathways can be used to boost type H vessel formation and osteogenesis. This might be of great importance for conditions involving compromised fracture healing or loss of bone mass. Ageing and post-menopausal estrogen deficiency are major risk factors for osteoporosis, and estrogen can promote angiogenesis15. Accordingly, decline of type H vessels and the concomitant reduction of osteoprogenitor cells could potentially offer a compelling explanation for the loss of bone mass during ageing and might enable therapeutic

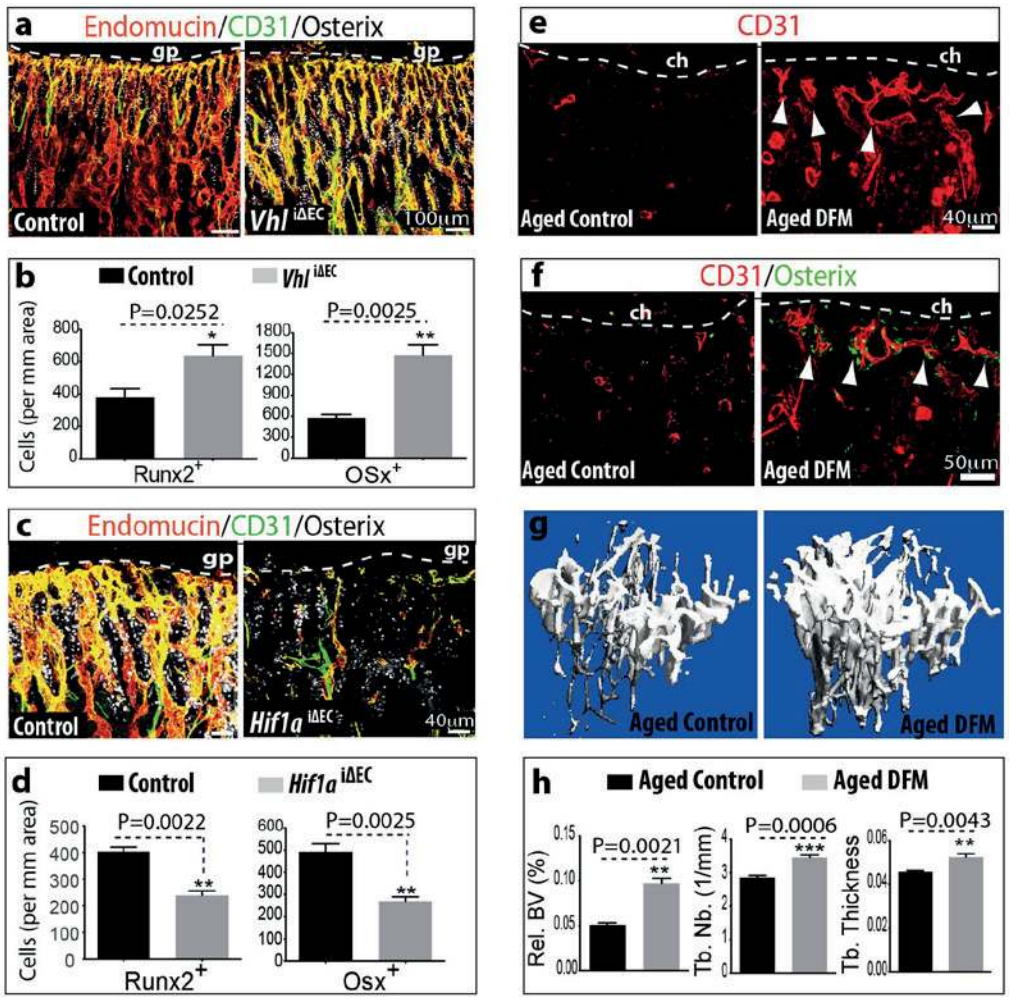

Figure 3. Type H ECs couple angiogenesis and osteogenesis.
a, Representative confocal images of CD31 (green), Endomucin (red) and Osterix (white) immunostained, 3 week-old VhliΔEC and control tibiae. b, Quantitation of Runx2+ and Osterix+ in VhliΔEC mutants and littermate controls. Data represent mean±s.e.m (n=5). P values, two-tailed unpaired t-test. c, Maximum intensity projections of 3 week-old Hif1aiΔEC and control tibia stained for CD31 (green), Endomucin (red) and Osterix (white). Growth plate, gp. d, Quantitation of Runx2+ and Osterix+ cells in Hif1aiΔEC mutant and control long bone. Data represent mean±s.e.m (n=5). P values, two-tailed unpaired t-test. e, f, Representative confocal images of CD31 (red, f) or CD31 and Osterix (green, g) stained tibia sections from aged DFM-treated and control mice. Low intensity projection shows only CD31hi cells. DFM induces CD31hi vessels and Osterix+ osteoprogenitors. Chondrocytes, ch. g, Representative μ-CT images of tibias from aged DFM-treated and control mice. h, Quantitative μ-CT analysis of relative bone volume (Rel. BV), trabecular number (Tb. Nb), and trabecular thickness (Tb. Thickness) in proximal tibia from aged DFM-treated and control mice. Data represent mean±s.e.m (n=5). P values, two-tailed unpaired t-test.

improvement of osteogenesis in elderly people.

About the author

Anjali P. Kusumbe (PhD)
Max Planck Institute for Molecular Biomedicine
Roentgenstrasse 20, 48149 Muenster, Germany
E-mail: anjali.kusumbe@mpi-muenster.mpg.de

03/2012 to Present: Postdoctoral fellow
Max Planck Institute for Molecular Biomedicine
Muenster, Germany
07/2005 – 01/2012: PhD student
National Center for Cell Science (NCCS), Pune, India
Department of Biotechnology (DBT), Government of India
Award of PhD degree (01/2013)
08/2004 - 06/2005: Junior Research Fellow
Indian Institute of Science, Bangaluru, India
08/2002 - 04/2004: Master of Science; Biotechnology
Hislop School of Biotechnology, Nagpur University, India
07/1999 - 07/2002: Bachelor of Science
Institute of Science, Nagpur University, India

Acknowledgements

I express my sincere gratitude to Prof. Dr. Ralf H. Adams for his invaluable scientific inputs and constant support. I am grateful to Saravana K. Ramasamy for his contribution to this work (equal contribution). Finally, I would like to thank all the members of Adams department.

References

1. Maes, C. et al. Increased skeletal VEGF enhances beta-catenin activity and results in excessively ossified bones. EMBO J 29, 424-441 (2010).
2. Glowacki, J. Angiogenesis in fracture repair. Clin. Orthop. Relat. Res. S82-89 (1998).
3. Burkhardt, R. et al. Changes in trabecular bone, hematopoiesis and bone marrow vessels in aplastic anemia, primary osteoporosis, and old age: a comparative histomorphometric study. Bone 8, 157-164 (1987).
4. Lu, C. et al. Effect of age on vascularization during fracture repair. J. Orthop. Res. 26, 1384-1389 (2008).
5. Wang, Y. et al. Ephrin-B2 controls VEGF-induced angiogenesis and lymphangiogenesis. Nature 465, 483-486 (2010).
6. Muzumdar, M. D., Tasic, B., Miyamichi, K., Li, L. & Luo, L. A global double-fluorescent Cre reporter mouse. Genesis 45, 593-605 (2007).
7. Nakashima, K. et al. The novel zinc finger-containing transcription factor osterix is required for osteoblast differentiation and bone formation. Cell 108, 17-29 (2002).
8. Lips, P., Courpron, P. & Meunier, P. J. Mean wall thickness of trabecular bone packets in the human iliac crest: changes with age. Calcif. Tissue Res. 26, 13-17 (1978).
9. Pugh, C. W. & Ratcliffe, P. J. Regulation of angiogenesis by hypoxia: role of the HIF system. Nat. Med. 9, 677-684 (2003).
10. Tang, N. et al. Loss of HIF-1alpha in endothelial cells disrupts a hypoxia-driven VEGF autocrine loop necessary for tumorigenesis. Cancer Cell 6, 485-495 (2004).
11. Tanimoto, K., Makino, Y., Pereira, T. & Poellinger, L. Mechanism of regulation of the hypoxia-inducible factor-1 alpha by the von Hippel-Lindau tumor suppressor protein. EMBO J 19, 4298-4309 (2000).
12. Jones, D. T. & Harris, A. L. Identification of novel small-molecule inhibitors of hypoxia-inducible factor-1 transactivation and DNA binding. Mol. Cancer Ther. 5, 2193-2202 (2006).
13. Wang, L. et al. Identification of a clonally expanding haematopoietic compartment in bone marrow. EMBO J 32, 219-230 (2013).
14. Ramasamy, S. K., Kusumbe, A. P., & Adams, R. H. Endothelial notch activity promotes angiogenesis and osteogenesis in bone. Nature 507, 376-380 (2014).
15. Losordo, D. W. & Isner, J. M. Estrogen and angiogenesis: A review. Arterioscler. Thromb. Vasc. Biol. 27, 255-65 (2001).